



Electronic properties of functionalized (5,5) beryllium oxide nanotubes



Ernesto Chigo Anota^{a,*}, Gregorio Hernández Cocoltzi^b

^a Benemérita Universidad Autónoma de Puebla, Facultad de Ingeniería Química, Ciudad Universitaria, San Manuel, Puebla, Código Postal 72570, Mexico

^b Benemérita Universidad Autónoma de Puebla, Instituto de Física 'Luis Rivera Terrazas', Apartado Postal J-48, Puebla 72570, Mexico

ARTICLE INFO

Article history:

Accepted 29 March 2013

Available online 6 April 2013

Keywords:

Beryllium oxide nanotubes

Hydroxyl

Point defects

Work function

DFT theory

ABSTRACT

Using the density functional theory (DFT) we study the structural and electronic properties of functionalized (5,5) chirality single wall beryllium oxide nanotubes (SW-BeONTs), i.e. armchair nanotubes. The nanotube surface and ends are functionalized by the hydroxyl (OH) functional group. Our calculations consider the Hamprecht–Cohen–Tozer–Handy functional in the generalized gradient approximation (HCTH-GGA) to deal with the exchange–correlation energies, and the base function with double polarization (DNP). The geometry optimization of both defects free and with point defects nanotubes is done applying the criterion of minimum energy. Six configurations are considered: The OH oriented toward the Be (on the surface and at the end), toward the O (on the surface and at the end) and placed at the nanotube ends. Simulation results show that the nanotube functionalization takes place at the nanotube ends with the Be–O bond displaying hydrogen-like bridge bonds. Moreover the nanotube semiconductor behavior remains unchanged. The polarity is high (it shows a transition from covalent to ionic) favoring solvation. On the other hand, the work function low value suggests this to be a good candidate for the device fabrication. When the nanotube contains surface point defects the work function is reduced which provides excellent possibilities for the use of this material in the electronic industry.

© 2013 Elsevier Inc. All rights reserved.

1. Introduction

Since the carbon nanotubes discovery by Iijima [1] these 1D structures have attracted the attention of the scientific community, they have been investigated both theoretically and experimentally. Similar studies have been performed on boron nitride nanotubes [2,3], zinc oxide nanotubes [4–8] and nanosheets [9,10]. However less attention has been paid to the earth alkaline compounds such as the 2D beryllium oxide (BeO) which was predicted to exist by Continenza et al. [11] in 1990. BeO nanosheets display graphene-like hexagonal configuration with sp^2 hybridization. Simulation studies on the BeO nanosheets by Baumeier et al. [12] and Wu et al. [13] have demonstrated that the pristine nanosheets behave as semiconductors however when they are fluorinated and hydrogenated [14] transform into semimetal. At the same time Baumeier et al. [12] have predicted the single wall BeO nanotubes (BeONTs) formation with semiconductor behavior and wide band gap in the interval of [7.3,8.8] eV for different chiralities (zig–zag and armchair structures). It is important to remark that these BeONTs display properties which are helicity independent. Studies on BeONTs [15]

doped with carbon and nitrogen considering different chiralities show energy gap reductions from 5.59 eV for pristine (6,6) BeONT, to 1.1 for BeONT:B, to 1.5 for BeONT:C and to 1.0 eV for BeONT:N. At the same time the beryllium vacancies induce an increase in the magnetic moment. As it stands doped BeONTs may be applied technologically in the spintronic industry. Therefore in this work we address the study of structural (bond lengths and nanotube diameters) and electronic properties (polarity, chemical potential and work function) of single wall (5,5) BeONTs. The nanotubes are considered in the armchair configuration and functionalized at the ends and surface by the hydroxyl group (OH). The choice of (5,5) chirality is because this structure exhibits a strain energy of 0.058 eV/atom which is low compared with other chiralities such as the $(n,0)$. This energy value indicates that the nanostructure may easily phase transform from 2D to 1D [12]. We also analyze the point defect effects on the BeONT–OH properties by paying attention on the vacancies of Be and O. Our studies are done using molecular simulation (local properties) within the density functional theory in order to explore possible applications in molecular sensing or field emission devices.

2. Simulation models and methods

First principles total energy calculations are performed to study (5,5) SW-BeONTs–OH structural and electronic properties. To deal

* Corresponding author. Tel.: +52 222 2 29 55 00.

E-mail addresses: ernesto.chigo@correo.buap.mx, echigoa@yahoo.es (E. Chigo Anota).

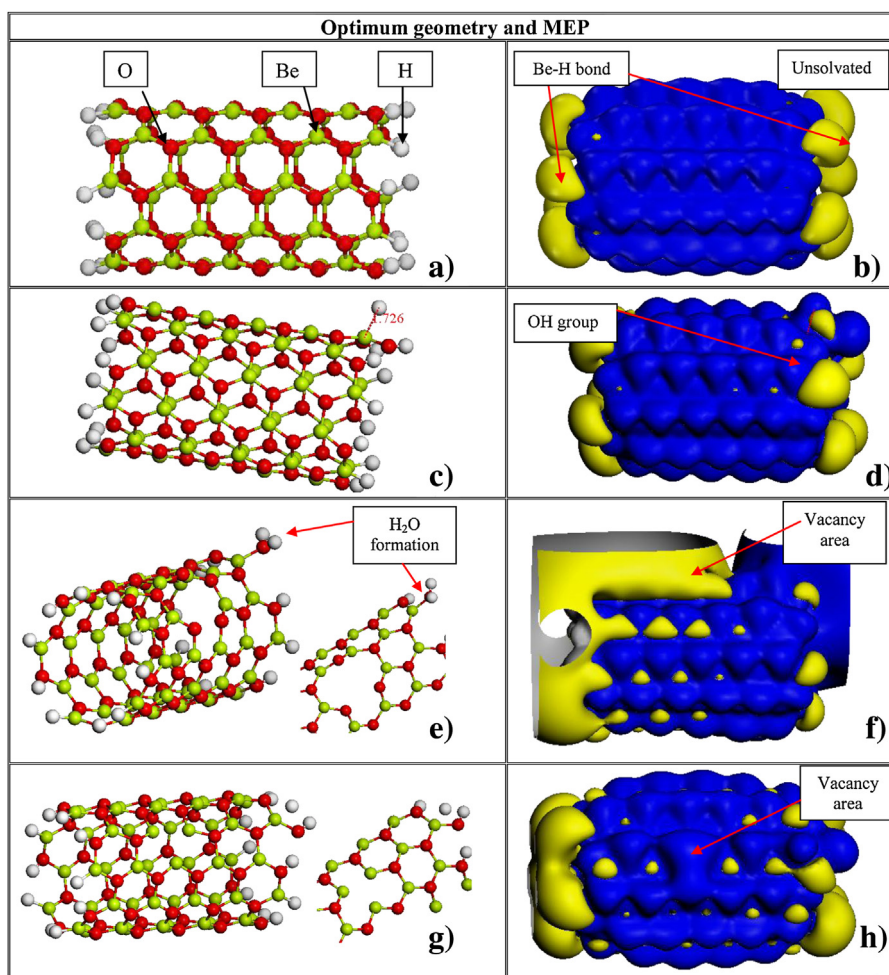


Fig. 1. This figure shows optimized structure for (a) pristine BeONT, (b) MEP for BeONT, (c) BeONT–OH, (d) MEP for BeONT–OH, (e) BeONT–OH with beryllium mono-vacancies, (f) MEP for BeONT–OH with beryllium mono-vacancies, (g) BeONT–OH with oxygen mono-vacancies, and (h) MEP for BeONT–OH with oxygen mono-vacancies. Yellow, red and white spheres represent Be, O and H, respectively. Blue color is for the positive charge and yellow color is for the negative charge.

with the exchange–correlation energies we apply the functional of Hamprecht–Cohen–Tozer–Handy (HCTH) [16] within the generalized gradient approximation (GGA). The base function DNP with double polarization [17] (we use a p -orbital for H, and a d -orbital for Be and O) is used as implemented in the quantum chemistry DMol³ code [18]. Six OH orientations have been investigated: In (C1) the fragment is oriented toward a Be, in (C2) the fragment is oriented toward an O, in (C3) the molecule is within the central hexagon of the surface, in (C4) the OH is at the nanotube end making a bond with Be, in (C5) the OH is at the nanotube end making a bond with a O and in (C6) the fragment is on the nanotube closed end, at the center of the cover. Charge neutrality and multiplicity 1 have been taken into account for both pristine BeONT and BeONT–OH structures. Simulations have been done considering the armchair model for the (5,5) SW-BeO nanotubes with length of 1.42 nm and diameter of 0.76 nm for the end mono-hydrogenated nanotubes (nanotube with open ends, Fig. 1a). The nanotube structure is composed of 120 atoms (50 Be, 50 O and 20 H) and the hydroxyl functional group contains 2 atoms.

Calculations have been also done to determine the chemical potential using the formula $(\text{HOMO} + \text{LUMO})/2$ provided (analogue) the Fermi level corresponds to that of the electron gas and it is at the middle of the energy gap. The work function is determined as the difference between the vacuum level (LUMO) and the Fermi level (chemical potential), this represents the minimum energy required to remove an electron from the Fermi level to the

vacuum level. The molecular electrostatic potentials (MEPs) surfaces have been determined as commonly reported in the literature [19]. We have employed a cut radius of 0.33 nm for the (OH) functional group and 0.40 nm for the single wall BeONT–OH structure with and without point defects, with a total energy convergence tolerance of 1.0×10^{-6} Ha. The structural stability has been dealt with the criterion of non complex vibration frequency [20].

3. Results and discussion

It is important to remark that 1D BN nanotubes, with open ends and saturated by N and B atoms instead of H atoms, are suitable systems to perform molecular simulations as already demonstrated by Hao et al. [21] in 2006. Hao et al. investigated the BN nanotubes magnetic properties with results showing variations produced by the saturation process. Moreover there exist reports showing that the most stable BN nanotubes configurations correspond to the (n,n) [22] geometries. This fact is supported by the possible synthesis of such nanotubes with open ends [23]. BN nanotubes of short length may be functionalized by polymers making them suitable for applications in biomedicine and to form composites with high mechanical resistance [3,4]. These results motivate the study of structural and electronic properties of functionalized SW-BeONTs as earlier reported by Chigo et al. [24–27].

Table 1
Relative and adsorption energy for systems BeONT–OH.

Configurations	Energy difference (eV/atom)	Adsorption energy (eV)
BeONT–OH		
C1	2.15×10^{-5}	−0.97
C2	1.96×10^{-4}	−0.96
C3	0.103	−0.94
C4	0.044	−11.66
C5	0.157	−17.00
C6	0.0	−2.13

3.1. Structural analysis

We have performed geometry optimization (see Table 1) using the above-discussed criteria. Results show that the hydroxyl functional group interactions with the SW-BeO nanotube yield the configuration C6 as the most stable geometry (Fig. 1c). The structure corresponds to the OH group bonded to the nanotube at the end of the open structure, in agreement with the work of Zhao and Ding [28]. This result is contrary to the Chigo et al. [24,26,27] findings for BN nanotubes. It is important to note that some metastable configurations of the BeONT–OH systems produce a small diameter contraction. These geometrical changes allow the hydroxyl group to interact with the pristine nanotube surface at a distance of 1.56 Å measure from the nanotube end. The structure displays a hydrogen-like bond between the Be and a O which are separated 1.73 Å of distance (Fig. 1c). Meanwhile in the nanotube the Be–O bond length remains constant with value of 1.57 Å, in agreement with the results obtained for pristine BeO nanotubes (Table 2). Calculation of the OH adsorption energy on the SW-BeO nanotube ($E_{ad} = E_{BeONT+OH} - E_{BeONT} - E_{OH}$) yields −2.13 eV (chemisorptions) which indicates an exothermic reaction.

3.2. Analysis of the electronic properties

The molecular electrostatic potential surfaces, MEPs (Fig. 1b and d), of both non- and functionalized nanotubes indicate how the electronic charge distribution is affected by the approaching of the hydroxyl group to the BeONT end. This induces small charge changes in the nanotube however the structure keeps the negative charge zone which means that the nanotube ends are highly reactive (zone with negative charge indicated in yellow). Note that the BeONT–OH system keeps the pristine BeONT properties and localizes the charge density near the Be atoms. It is remarkable how the MEPs surfaces exhibit zones with high charge density concentration at the nanotube ends instead of the surface as it happens in the SW-BNNTs [24]. Results induce us to conclude that the dispersion of such nanostructures is possible. When some amount of nanotubes are placed in vacuum or in some organic solvent with net negative charge, the repulsion will be stronger; this fact may be used to explore new technological applications.

Recall that pristine BeONT exhibits semiconductor behavior with large energy gap (6.20 eV), according to the energy difference between the HOMO and LUMO orbitals. This gap is drastically reduced to 1.92 eV for the BeONT–OH, however the modified system keeps the semiconductor characteristics. The polarity of 0 D for the pristine BeONT is increased to 2.15 D for the BeONT–OH structure. At the same time there is a transition from a covalent (BeONT) to an ionic (BeONT–OH) characteristics. The charge distribution is localized at the interaction zone between the nanotube end and the OH group, as depicted by the MEPs (Fig. 1d). The polarity increase is also obtained in BN nanotubes with different chiralities [29] and BN nanosheets [30] interacting with the chitosan biopolymer. The tendency to increase the polarity suggests the possibility to solvate the nanotubes which are functionalized by the OH group. This is in a similar fashion as in the BNNTs solvated in water,

which are functionalized by methoxy-poly (ethylene glycol)-1,2-distearoyl-sn-glycero-3-phosphoethanolamine-N, already reported in the literature [3]. The polarity increase is also obtained in BN [24,26,27,29,31] and SiC [25] nanotubes functionalized by molecules or functional groups. Calculations of the work function yield a value of 3.1 eV for pristine BeONT and a value of 0.96 eV for BeONT–OH, which indicate that the electron charge transfer is favored in the latter system. The presence of adsorbates at the nanotube ends induces optimal conditions to improve field emission properties (FEPs) as already reported in the literature for BN nanotubes functionalized by triatomic water molecules or oxygen molecules [28]. FEPs have been improved since the potential barrier has been reduced by the OH adsorbed at the BeONT ends instead of the surface; this indicates the viability for the system to be considered as a good candidate for technological applications in spintronics and sensor devices.

Finally we explore the electric conductivity changes as obtained through the formula $\sigma \propto \exp(-E_g/kT)$, where k is the Boltzmann constant and T the temperature [32]. By considering a temperature the BeONT–OH exhibits a small energy gap (1.92 eV in vacuum) and improved conductivity meanwhile pristine BeONT exhibits a large energy gap and small conductivity which induce a good kinetic stability in vacuum.

3.3. Influence of point defects

Lattice defects such as vacancies in nanotubes are possible to generate experimentally as already done in BNNTs [33]. Since vacancies produce changes in the nanotube electronic properties we study oxygen and beryllium mono-vacancies in pristine and functionalized BeONTs. In the presence of Be mono-vacancies the nanotube lattice does not reconstruct (Fig. 1e), under these conditions the geometric parameters are unchanged. Similar situation takes place in the SW-BeONT functionalized by the OH group. However in the BeONT–OH structures the structural changes are more evident they produce an increase in the OH and BeONT bond length by 0.15 Å with a final value of 1.70 Å. In this case H₂O molecules are formed with the H–O–H configuration displaying an angle of 108.64° and bond length of 0.96 Å (Fig. 1e). The angle and bond length values agree well with those reported in the literature for boron nitride oxide nanosheets, where the OH groups combine to form water molecules [34]. Concerning the electronic properties, we find similar values of the energy gap between the HOMO and LUMO orbitals of the pristine BeONT and BeONT–OH structures. This is because both structures transform from semiconductor to semimetal (see Table 2) with the transition been produced by the vacancy instead of the functionalization. These results agree well with those obtained by Gorbunova et al. [15]. The work function small values of both nanotubes suggest that these structures may be used to fabricate devices such as displays.

Furthermore, the most striking change induced by the vacancies is the variation of the dipole moment, which takes a new value of 4.23 D for the pristine BeONT and 26.59 D for the BeONT–OH. The dipole variations produce electron polarization, and allow the possible solubility and dispersion of the nanotubes. It is important to remark changes in the BeONT structure when this is affected by the presence of vacancies, its chemical reactivity (arithmetic average between frontier orbitals) lowers from −3.68 to −6.57 eV. Similarly in the BeONT–OH structure the chemical reactivity reaches the value of −5.28 eV. Taking into account these values of chemical reactivity we may conclude that nanotubes exhibit low toxicity.

In the presence of oxygen mono-vacancies both BeONT–OH and pristine BeONT (Fig. 1g) do not reconstruct near the vacancy zone (Fig. 1f). The vacancy hole is of smaller size as compared with the previous case of the Be vacancy. The structural changes induced by

Table 2

In this table we report optimized structural parameters and electronic properties: HOMO–LUMO energy gap, Fermi energy, polarity and work function of the BeONT–OH structure.

Systems	Bond length (Å)		HOMO–LUMO gap (eV)	Energy Fermi level (eV)	Dipolar moment (Debye)	Work function (eV)
	Be–O	O–H				
(5,5) BeONT ^a			7.75 [3] 7.07 [35]		0.0 [35]	
hBeO Nanosheet	1.52 [3] 1.525 [4]		5.73 [3] 5.45 [4]			
—						
(5,5) BeONT	1.57		6.20	−3.68	0.0	3.1
(5,5) BeONT vacancy of Be	1.57		0.41	−6.57	4.23	0.21
(5,5) BeONT vacancy of O	1.57		4.55	−3.53	0.23	2.27
OH			5.98		1.68	
(5,5) BeONT–OH	1.57	0.96	1.92	−5.55	2.15	0.96
(5,5) BeONT–OH vacancy of O	1.56	0.96	1.19	−3.95	1.65	0.6
(5,5) BeONT–OH vacancy of Be	1.54	0.96	0.16	−5.28	26.59	0.082

^a Diameter = 0.73 nm.

these vacancies are unimportant. Meanwhile the chemical reactivity remains constant in the presence of O vacancy in both pristine BeONT and BeONT–OH systems indicating relative stability. The increase in the polarity suggests the possibility of solvation and dispersion. At the same time according to the decrease in the energy gap these structures are good candidates to improve field emission properties.

The MEPs of these systems with Be vacancies (Fig. 1f and h) display notable changes in the charge distribution in contrast

to the oxygen vacancies. This analysis of the charge redistribution complements the HOMO and LUMO isosurface study (Fig. 2) where the p_z and s orbital hybridization of Be and O is observed at the vacancy zone. However in the BeONT system is observed the contribution of either oxygen or beryllium. When BeONT–OH contains Be vacancies the energy gap decreases indicating that vacancies may favor the charge transport, however in the case of oxygen vacancies the structure is only thermal stabilized.

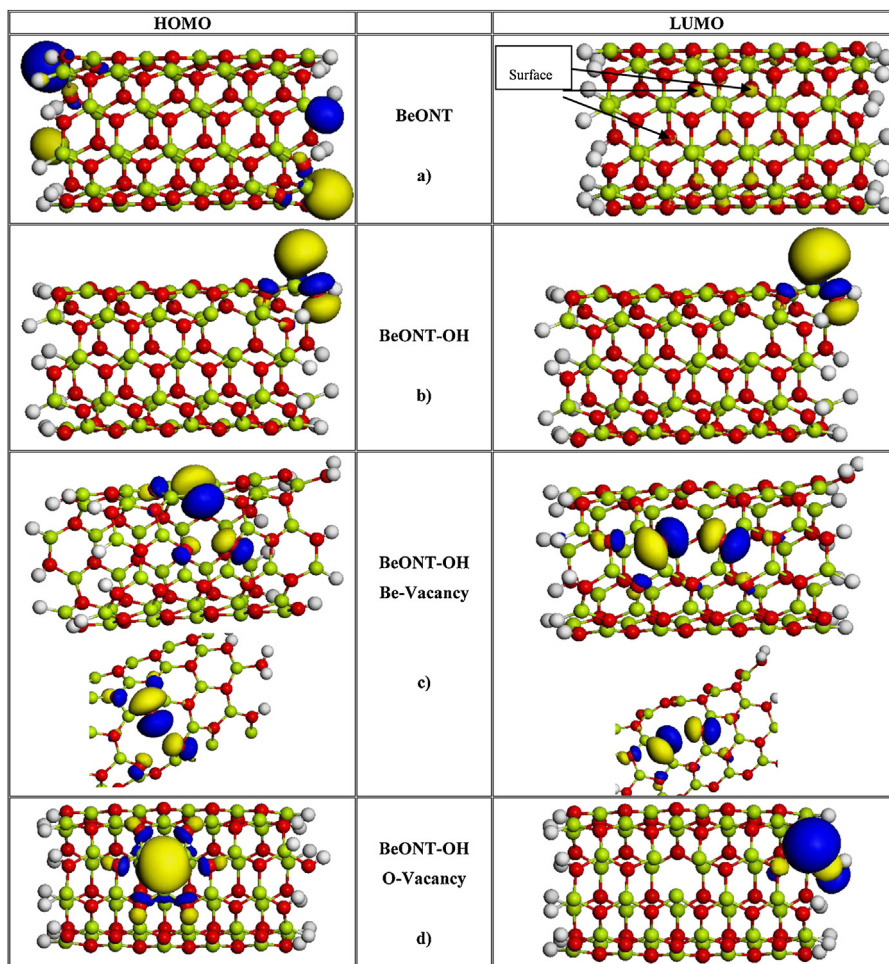


Fig. 2. The figure displays HOMO and LUMO isosurfaces for (a) pristine BeONT, (b) BeONT–OH in the optimized configuration, (c) BeONT–OH with beryllium mono-vacancies, and (d) BeONT–OH with oxygen mono-vacancies.

4. Conclusions

We have presented *ab-initio* studies of the interaction between the OH functional group and (5,5) single wall beryllium oxide nanotubes. Results show that the 1D structure may be functionalized by the OH group at the nanotubes ends through the Be atom in a chemical process. The OH interaction with the BeONT (in the absence of defects and with defects) induces an increase in the polarity which in turn produces the possible solvation and dispersion of the nanotubes, suggesting the possibility of applications in the biochemical industry. The Be mono-vacancy lowers the reactivity and allows the formation of the H₂O molecule at the nanotubes ends where the OH is chemisorbed, indicating a possible route for obtaining water. On the other hand, mono-vacancies modify the energy gap inducing a transition from a semiconductor to a semimetal, which may favor the technological applications in spintronics. In addition due to the small work function these nanostructures are good candidates to improve the field emission phenomenon.

Acknowledgments

This work was partially supported by projects: VIEP-BUAP (CHAE-ING13-G), Cuerpo Académico Ingeniería en Materiales (BUAP-CA-177), Cuerpo Académico Física Computacional de la Materia Condensada (BUAP-CA-194) and VIEP-BUAP-EXC11-G.

References

- [1] S. Iijima, Helical microtubules of graphitic carbon, *Nature* 354 (1991) 56–58.
- [2] A. Rubio, J.L. Corkill, M.L. Cohen, Theory of graphitic boron nitride nanotubes, *Physical Review B* 49 (1994) 5081–5084.
- [3] X. Blasé, A. Rubio, S.G. Louie, M.L. Cohen, Stability and band gap constancy of boron nitride nanotubes, *Europhysics Letters* 28 (1994) 335–340.
- [4] Y.K. Tseng, C.J. Huang, H.M. Cheng, I.N. Lin, K.S. Liu, I.C. Chen, Characterization and field-emission properties of needle-like zinc oxide nanowires grown vertically on conductive zinc oxide films, *Advanced Functional Materials* 13 (2003) 811–814.
- [5] J.M. Bao, M.A. Zimmmer, F. Capasso, X.W. Wang, Z.F. Ren, Broadband ZnO single-nanowire light-emitting diode, *Nano Letters* 6 (2006) 1719–1722.
- [6] Q.H. Li, Y.X. Liang, Q. Wan, T.H. Wang, Oxygen sensing characteristics of individual ZnO nanowire transistors, *Applied Physics Letters* 85 (2004) 6389–6391.
- [7] Z.L. Wang, J.H. Song, Piezoelectric nanogenerators based on zinc oxide nanowire arrays, *Science* 312 (2006) 242–246.
- [8] J.C. Johnson, K.P. Knutsen, H.Q. Yan, M. Law, Y.F. Zhang, P.D. Yang, R.J. Saykally, Ultrafast carrier dynamics in single ZnO nanowire and nanoribbon lasers, *Nano Letters* 4 (2004) 197–204.
- [9] Y. Wang, Y. Ding, J. Ni, S. Shi, C. Li, J. Shi, Electronic structures of fully fluorinated and semifluorinated zinc oxide sheets, *Applied Physics Letters* 96 (2010) 213117–213119.
- [10] Q. Tang, Y. Li, Z. Zhou, Y. Chen, Z. Chen, Tuning electronic and magnetic properties of wurtzite ZnO nanosheets by surface hydrogenation, *ACS Applied Materials & Interfaces* 2 (2010) 2442–2447.
- [11] A. Continenza, R.M. Wentzcovitch, A.J. Freeman, Theoretical investigation of graphitic BeO, *Physical Review B* 41 (1990) 3540–3544.
- [12] B. Baumeier, P. Krüger, J. Pollmann, Structural, elastic, and electronic properties of SiC, BN, and BeO nanotubes, *Physical Review B* 76 (2007) 085407(1)–085407(10).
- [13] W. Wu, P. Lu, Z. Zhang, W. Guo, Electronic and magnetic properties and structural stability of BeO sheet and nanoribbons, *ACS Applied Materials & Interfaces* 3 (2011) 4787–4795.
- [14] Y.Y. Wang, Ding Electronic structure of fluorinated and hydrogenated beryllium monoxide nanostructures, *Physica Status Solidi: Rapid Research Letters* 6 (2012) 83–85.
- [15] M.A. Gorbunova, I.R. Shein, Yu.N. Makurin, V.V. Ivanovskaya, V.S. Kijko, A.L. Ivanovskii, Electronic structure and magnetism in BeO nanotubes induced by boron, carbon and nitrogen doping, and beryllium and oxygen vacancies inside tube, *Physica E* 41 (2008) 164–168.
- [16] A.D. Boese, N.C. Handy, A new parameterization of exchange–correlation generalized gradient approximation functional, *Journal of Chemical Physics* 114 (2001) 5497–5503.
- [17] B. Delley, An all-electron numerical method for solving the local density functional for polyatomic molecules, *Journal of Chemical Physics* 92 (1990) 508–517.
- [18] B. Delley, From molecules to solids with the DMol³ approach, *Journal of Chemical Physics* 113 (2000) 7756–7765.
- [19] J.J. Hernández Rosas, R.E. Ramírez Gutiérrez, A. Escobedo Morales, E. Chigo Anota, First principles calculations of the electronic and chemical properties of graphene, graphane, and graphane oxide structures, *Journal of Molecular Modeling* 17 (2011) 1133–1139.
- [20] J.B. Foresman, Æ. Frisch, *Exploring Chemistry with Electronic Structure Methods*, second ed., Gaussian Inc., USA, 70 (1996).
- [21] S. Hao, G. Zhou, W. Duan, J. Wu, B.L. Gu, Tremendous spin-splitting effects in open boron nitride nanotubes: application to nanoscale spintronic devices, *Journal of the American Chemical Society* 128 (2006) 8453–8458.
- [22] H.J. Xiang, J. Yang, J.G. Hou, Q. Zhu, First-principles study of small-radius single-walled BN nanotubes, *Physical Review B* 68 (2006) 035427(1)–035427(5).
- [23] D. Golberg, Y. Bando, Unique morphologies of boron nitride nanotubes, *Applied Physics Letters* 79 (2001) 415–417.
- [24] E. Chigo Anota, G. Hernández Coccoletzi, First-principles simulations of the chemical functionalization of (5,5) boron nitride nanotubes, *Journal of Molecular Modeling* (2013), <http://dx.doi.org/10.1007/s00894-013-1782-3>.
- [25] E. Chigo Anota, G. Hernández Coccoletzi, Influence of point defects on structural and electronic properties SiC nanotubes, *Mol. Simul.*, under review.
- [26] E. Chigo Anota, Interaction BN nanotubes – dioxin: influence of point defect on structural and electronic properties, *J. Mol. Model.*, under review.
- [27] E. Chigo Anota, H. Hernández Coccoletzi, M. Salazar Villanueva, D. García Toral, First-principles investigation of the interaction between BN, SiC and ZnO nanotubes–BaTiO₃, *J. Mol. Graphics Model.*, under review.
- [28] J.X. Zhao, Y.H. Ding, Theoretical studies of the interaction of an open-ended boron nitride nanotube (BNNT) with gas molecules, *Journal of Physical Chemistry C* 112 (2008) 20206–20211.
- [29] A. Rodríguez Juárez, E. Chigo Anota, H. Hernández Coccoletzi, A. Flores Riveros, Adsorption of chitosan on BN nanotubes: a DFT investigation, *Applied Surface Science* 268 (2013) 259–264.
- [30] E. Chigo Anota, L. D. Hernández Rodríguez, G. Hernández Coccoletzi, Influence of point defect on the adsorption of chitosan on BN nanosheets, *J. Mol. Model.*, under review.
- [31] E. Chigo Anota, G. Hernández Coccoletzi, Generalized gradient approximation-based analysis of the metformin adsorption on boron nitride nanotubes, *Appl. Surf. Sci.*, under review.
- [32] S. Li, *Semiconductor Physical Electronics*, Second ed., Springer, USA, 2006.
- [33] A. Zobelli, C.P. Ewels, A. Gloter, G. Seifert, O. Stephan, S. Csillag, C. Colliex, Defective structure of BN nanotubes: from single vacancies to dislocation lines, *Nano Letters* 6 (2006) 1955–1960.
- [34] E. Chigo Anota, A. Escobedo Morales, M. Salazar Villanueva, O. Vázquez Cuchillo, E. Rubio Rosas, On the influence of point defects on the structural and electronic properties of graphene-like sheets: a molecular simulation study, *Journal of Molecular Modeling* 19 (2013) 839–846.
- [35] A. Seif, E. Zahedi, G.M. Rozbahani, A computational investigation of carbon-doped beryllium monoxide nanotubes, *Central European Journal of Chemistry* 10 (1) (2012) 96–104.